AD-A047 764 AIR FORCE INST OF TECH WRIGHT-PATTERSON AFB OHIO F/G 17/10

AMPLITUDE DEPENDENT ERRORS IN THE CALCULATION OF WIENER KERNELS--ETC(U)

MAR 77 G R ELLIS

UNCLASSIFIED AFIT-CI-78-7 NL

| OF |

AD
A047 764

END

DATE FILMED

1 -78

DDC

AMPLITUDE DEPENDENT ERRORS IN THE CALCULATION OF WIENER KERNELS

BY

GARY ROBERT ELLIS

A THESIS PRESENTED TO THE GRADUATE COUNCIL OF
THE UNIVERSITY OF FLORIDA
IN PARTIAL FULFILLMENT OF THE REQUIREMENTS FOR THE
DEGREE OF MASTER OF ENGINEERING

UNIVERSITY OF FLORIDA

1977

UNCLASSIFIED
SECURITY CLASSIFICATION OF THIS PAGE (When Data Entered)

REPORT DOCUMENTATION PAGE		READ INSTRUCTIONS BEFORE COMPLETING FORM
1. REPORT NUMBER (14) AFIT-CI-78-7	2. GOVT ACCESSION NO.	3. RECIPIENT'S CATALOG NUMBER
4. TITLE (and Subtitle) (6) Amplitude Dependent Errors in the Calculation of Wiener Kernels.		5. TYPE OF REPORT & PERIOD COVERED Thesis
		6. PERFORMING ORG. REPORT NUMBER
7. AUTHOR(s) (10) 2d Lt Gary Robert Ellis		8. CONTRACT OR GRANT NUMBER(s) (9) Master's thesis,
9. PERFORMING ORGANIZATION NAME AND ADDRESS AFIT Student University of Florida, Gainesville FL		10. PROGRAM ELEMENT, PROJECT, TASK AREA & WORK UNIT NUMBERS
11. CONTROLLING OFFICE NAME AND ADDRESS AFIT/CI WPAFB OH 45433		12. REPORT DATE (11) March 1977
		13. NUMBER OF PAGES 44 Pages
14. MONITORING AGENCY NAME & ADDRESS(if different from Controlling Office) (12) 50p.		15. SECURITY CLASS. (of this report) Unclassified
		15a. DECLASSIFICATION/DOWNGRADING SCHEDULE

16. DISTRIBUTION STATEMENT (of this Report)

Approved for Public Release; Distribution Unlimited

17. DISTRIBUTION STATEMENT (of the abstract entered in Block 20, if different from Report)

18. SUPPLEMENTARY NOTES

APPROVED FOR PUBLIC RELEASE AFR 190-17.

JERRAL F. GUESS, Captain, USAF
Director of Information, AFIT

19. KEY WORDS (Continue on reverse side if necessary and identify by block number)

20. ABSTRACT (Continue on reverse side if necessary and identify by block number)

DD FORM 1 JAN 73 1473 EDITION OF 1 NOV 65 IS OBSOLETE

012 200

UNCLASSIFIED
SECURITY CLASSIFICATION OF THIS PAGE (When Data Entered)

SECURITY CLASSIFICATION OF THIS PAGE(When Data Entered)

SECURITY CLASSIFICATION OF THIS PAGE(When Data Entered)

INSTRUCTIONS FOR PREPARATION OF REPORT DOCUMENTATION PAGE

RESPONSIBILITY. The controlling DoD office will be responsible for completion of the Report Documentation Page, DD Form 1473, in all technical reports prepared by or for DoD organizations.

CLASSIFICATION. Since this Report Documentation Page, DD Form 1473, is used in preparing announcements, bibliographies, and data banks, it should be unclassified if possible. If a classification is required, identify the classified items on the page by the appropriate symbol.

COMPLETION GUIDE

General. Make Blocks 1, 4, 5, 6, 7, 11, 13, 15, and 16 agree with the corresponding information on the report cover. Leave Blocks 2 and 3 blank.

Block 1. Report Number. Enter the unique alphanumeric report number shown on the cover.

Block 2. Government Accession No. Leave Blank. This space is for use by the Defense Documentation Center.

Block 3. Recipient's Catalog Number. Leave blank. This space is for the use of the report recipient to assist in future retrieval of the document.

Block 4. Title and Subtitle. Enter the title in all capital letters exactly as it appears on the publication. Titles should be unclassified whenever possible. Write out the English equivalent for Greek letters and mathematical symbols in the title *(see "Abstracting Scientific and Technical Reports of Defense-sponsored RDT/E,"AD-667 000)*. If the report has a subtitle, this subtitle should follow the main title, be separated by a comma or semicolon if appropriate, and be initially capitalized. If a publication has a title in a foreign language, translate the title into English and follow the English translation with the title in the original language. Make every effort to simplify the title before publication.

Block 5. Type of Report and Period Covered. Indicate here whether report is interim, final, etc., and, if applicable, inclusive dates of period covered, such as the life of a contract covered in a final contractor report.

Block 6. Performing Organization Report Number. Only numbers other than the official report number shown in Block 1, such as series numbers for in-house reports or a contractor/grantee number assigned by him, will be placed in this space. If no such numbers are used, leave this space blank.

Block 7. Author*(s)*. Include corresponding information from the report cover. Give the name*(s)* of the author*(s)* in conventional order *(for example, John R. Doe or, if author prefers, J. Robert Doe)*. In addition, list the affiliation of an author if it differs from that of the performing organization.

Block 8. Contract or Grant Number*(s)*. For a contractor or grantee report, enter the complete contract or grant number*(s)* under which the work reported was accomplished. Leave blank in in-house reports.

Block 9. Performing Organization Name and Address. For in-house reports enter the name and address, including office symbol, of the performing activity. For contractor or grantee reports enter the name and address of the contractor or grantee who prepared the report and identify the appropriate corporate division, school, laboratory, etc., of the author. List city, state, and ZIP Code.

Block 10. Program Element, Project, Task Area, and Work Unit Numbers. Enter here the number code from the applicable Department of Defense form, such as the DD Form 1498, "Research and Technology Work Unit Summary" or the DD Form 1634. "Research and Development Planning Summary," which identifies the program element, project, task area, and work unit or equivalent under which the work was authorized.

Block 11. Controlling Office Name and Address. Enter the full, official name and address, including office symbol, of the controlling office. *(Equates to funding/sponsoring agency. For definition see DoD Directive 5200.20, "Distribution Statements on Technical Documents.")*

Block 12. Report Date. Enter here the day, month, and year or month and year as shown on the cover.

Block 13. Number of Pages. Enter the total number of pages.

Block 14. Monitoring Agency Name and Address *(if different from Controlling Office)*. For use when the controlling or funding office does not directly administer a project, contract, or grant, but delegates the administrative responsibility to another organization.

Blocks 15 & 15a. Security Classification of the Report: Declassification/Downgrading Schedule of the Report. Enter in 15 the highest classification of the report. If appropriate, enter in 15a the declassification/downgrading schedule of the report, using the abbreviations for declassification/downgrading schedules listed in paragraph 4-207 of DoD 5200.1-R.

Block 16. Distribution Statement of the Report. Insert here the applicable distribution statement of the report from DoD Directive 5200.20, "Distribution Statements on Technical Documents."

Block 17. Distribution Statement *(of the abstract entered in Block 20, if different from the distribution statement of the report)*. Insert here the applicable distribution statement of the abstract from DoD Directive 5200.20, "Distribution Statements on Technical Documents."

Block 18. Supplementary Notes. Enter information not included elsewhere but useful, such as: Prepared in cooperation with . . . Translation of *(or by)* . . . Presented at conference of . . . To be published in . . .

Block 19. Key Words. Select terms or short phrases that identify the principal subjects covered in the report, and are sufficiently specific and precise to be used as index entries for cataloging, conforming to standard terminology. The DoD "Thesaurus of Engineering and Scientific [illegible]s" *(TEST)*, AD-672 000, can be helpful.

Block 20. Abstract. [illegible]act should be a brief *(not to exceed 200 words)* factual summary of the most significant information contained in the report. [illegible], the abstract of a classified report should be unclassified and the abstract to an unclassified report should consist of publ[illegible]ible information. If the report contains a significant bibliography or literature survey, mention it here. For information on prepa[illegible]stracts see "Abstracting Scientific and Technical Reports of Defense-Sponsored RDT&E," AD-667 000.

☆ U.S. GOVERNMENT PRINTING OFFICE : 1973–729-091/1431 3-1

ACKNOWLEDGMENTS

This research was first suggested by the efforts of Dr. James G. Constantine and Lt. Col. Raymond B. Walker in the Mines Branch, Air Force Armament Laboratory, who were also responsible for the collection and processing of much of the experimental data. Dr. William E. Brownell and Mr. Darrel J. Duffy in the Department of Neuroscience and Surgery (ENT), University of Florida provided computational facilities and programming assistance. The aid of these individuals is gratefully acknowledged. Special thanks is given to Dr. Michael E. Warren in the Department of Electrical Engineering, University of Florida, and the chairman of the author's committee, without whose instruction and encouragement this thesis would not have been possible.

TABLE OF CONTENTS

Abstract of Thesis Presented to the Graduate Council
of the University of Florida in Partial Fulfillment
of the Requirements for the Degree of Master of Engineering

AMPLITUDE DEPENDENT ERRORS IN
THE CALCULATION OF WIENER KERNELS

By

Gary Robert Ellis

March, 1977

Chairman: Dr. Michael E. Warren
Major Department: Electrical Engineering

The calculation of Wiener kernels via the cross-correlation methods of Lee and Schetzen for use in nonlinear system identification is examined. The calculated kernels are shown to depend upon the power of the input approximating a white noise probe. This dependence is due to amplitude related nonlinearities such as thresholds in the system, and is also a consequence of the finite computations used to derive the kernels. Data obtained from investigations into near field seismic energy propagation is used to calculate kernels identifying the propagation medium, and the effects of the input power level on the calculated kernels are shown.

Chairman

CHAPTER I

INTRODUCTION

There has long been an interest in discriminating among different types of seismic energy sources via detection and classification of the signals they emit. This has generally been facilitated by using linear models for seismic propagation channels. Good models have been developed for some cases, such as earthquakes or underground explosions, where sensing devices are at a considerable distance from the source (see White, 1965). In the near field, however, these models have been less than satisfactory. Walker (1976) shows this is at least partly due to drastic nonlinearities which are introduced into the dynamics of the near field propagation channel. These nonlinearities result from the coupling over a large area of acoustic energy also emitted from the source into the seismic propagation medium, and they must be identified in order to devise accurate near field models of the medium.

Several methods, such as phase-plane and describing function techniques, are available for nonlinear system analysis, but these methods are specialized and can only be applied to narrow classes of nonlinear systems. Volterra (1930) was the first to suggest a general method for nonlinear system analysis when he introduced the concept of expanding the output of a time invariant nonlinear system into a series of multidimensional convolutions known as Volterra functionals

$$y(t) = K_0 + \sum_{n=1}^{\infty} \int_{-\infty}^{\infty} \cdots \int_{-\infty}^{\infty} K_n(\tau_1,\ldots,\tau_n)x(t-\tau_1)\ldots x(t-\tau_n)d\tau_1\ldots d\tau_n \ . \tag{1.1}$$

From this concept there has grown a powerful and general method for characterizing time invariant nonlinear systems known as the Wiener Theory.

Wiener (1958) showed that the proper probe for studying such nonlinear systems is a zero-mean white Gaussian process. He, therefore, modified Volterra's representation to

$$y(t) = \sum_{n=0}^{\infty} G_n[h_n, x(t)] \ , \tag{1.2}$$

where the G-functionals, $\{G_n\}$, are a complete set of orthogonal functionals when $x(t)$ is a zero-mean white Gaussian process:

$$\overline{G_m[h_m, x(t)]G_n[h_n, x(t)]} = 0 \ , \quad m \neq n \ . \tag{1.3}$$

(The overbar indicates the time average over the interval $(-\infty,\infty)$.) The functions $h_n(\tau_1,\ldots,\tau_n)$ are known as the Wiener kernels and they completely characterize the system. Basically, the Wiener theory requires the measurement of the system response to the zero-mean white Gaussian input probe. Then, due to the orthogonality of the G-functionals, the mathematical relationships between the response and the probe can be used to calculate the Wiener kernels.

Wiener (1958) presented a method for making this calculation that employs a further expansion of the kernels into orthogonal functions such as Laguerre polynomials. This method, however, is not in common use, since practical considerations do not permit infinite expansions of the kernels. Kernels calculated in this manner using finite expansions approximate the actual kernels in a minimum integral square sense. In addition, Wiener's method is suitable for analog implementation, but it does not readily lend itself to digital implementation.

Lee and Schetzen (1965) introduced an algorithm for determining the Wiener kernels which employs cross-correlation techniques. It avoids the expansion of the kernels into orthogonal functions which is essential in Wiener's method, and allows the kernels to be calculated point by point for simple digital implementation. Other algorithms and modifications to the Wiener theory have been presented. French and Butz (1973) proposed an algorithm which reduces computing time with some loss of high frequency information through the use of Fast Fourier Transforms. Krausz (1974) modified the Wiener theory for use with Poisson distributed discrete input probes. Promising research is currently underway at the California Institute of Technology by Fender (see Brownell, 1976) which employs computational ideas similar to those of Krausz to construct hardware that very efficiently calculates Wiener kernels for certain classes of biological phenomena. A brief review of the Wiener theory and especially the method of Lee and Schetzen which is employed in this research is presented in Chapter II.

Walker, Constantine and Warren (1976) investigated the feasibility of using the Wiener theory of nonlinear system identification to develop near field models for seismic energy propagation media. The models thus devised showed significant improvement over the linear models (see Walker, 1976). During this investigation, however, it was noted that the calculated kernels displayed certain dependencies upon the power level of the input probe. Further examinations revealed this phenomenon to be due to both the amplitude related nonlinearities in the system such as thresholds and to the approximations of white Gaussian noise used in the actual processing involved in calculating the kernels. Since the kernels are calculated by probing the system at a single constant power level the

amplitude dependencies due to these two factors reflect themselves as errors in the kernels. The primary focus of this research is the examination of these amplitude dependent errors in the calculation of the Wiener kernels.

A good example of the amplitude dependencies exhibited by the calculated kernels for systems with thresholds is the simple limiter. Such a system will appear to change its nonlinear characteristics depending upon the amplitude of the input signal. If the amplitude is small compared to the threshold of the limiter, the system will appear linear. On the other hand, if the input amplitude is large compared with the threshold, the system takes on the appearance of a hard limiter which is quite nonlinear. Even though the algorithms for calculation of Wiener kernels involve normalization with respect to the input power level, the effects of such amplitude dependent nonlinearities will be reflected in the calculated kernels depending upon the power level of the input probe. This particular problem together with the errors involved in approximating a Gaussian white process are discussed in Chapter III.

The amplitude dependencies in the kernels due to the calculation processes result from the finite as opposed to infinite computations used to derive the kernels. The Wiener theory requires that averages be taken over infinite intervals which also implies that the zero-mean white Gaussian input probe must have infinite length. This, of course, is impossible in a practical application of the theory and infinite intervals are approximated by long finite intervals. This creates a problem when, during the course of calculating the kernels, the means of random processes do not equal their sample means over finite intervals. This has the effect of introducing biases into the input probe, and as discussed by Marmarelis

(1972) may cause considerable errors in cases where, theoretically, terms containing the average of the process should drop out. This problem is discussed in Chapter IV.

Chapter V presents a practical example of the problems which are encountered due to these two types of dependencies when calculating the Wiener kernels. A seismic energy propagation medium was probed with zero-mean white Gaussian processes at various power levels. Kernels were calculated for each of the various probes used and the effects of the probe's power level on the calculated kernel are discussed. Chapter VI contains a summary of the results of this research and suggestions for further work in this area.

CHAPTER II

REVIEW OF THE WIENER THEORY

The problem of finding the relationship that determines the output of a system in response to any relevant input is known as system identification. A variety of well-known techniques exist for the identification of linear systems, but identification techniques applicable to broad classes of nonlinear systems are lacking. Several methods for nonlinear system identification are available, such as phase-plane and describing function techniques, but they have serious limitations and are useful only for narrow classes of systems. There is, however, a fairly general theory which has grown from the work in this area by Norbert Wiener.

Volterra (1930) introduced an input-output relationship as a series of multidimensional convolutions (see eqn.(1.1)). Prompted by Volterra's work, Wiener (1958) laid the foundation for a general theory for nonlinear systems by demonstrating that the proper probe for studying such systems is a zero-mean white Gaussian process. With this in mind, he modified the Volterra series to

$$y(t) = \sum_{n=0}^{\infty} G_n[h_n, x(t)] \, , \tag{2.1}$$

where $\{G_n\}$ is a complete set of functionals which are orthogonal (see eqn. (1.3)) when $x(t)$ is a zero-mean white Gaussian process. Each G-functional, G_n, is the sum of the nth degree homogeneous functional

$$\int_{-\infty}^{\infty}\cdots\int_{-\infty}^{\infty} h_n(\tau_1,\ldots,\tau_n)x(t-\tau_1)\ldots x(t-\tau_n)d\tau_1\ldots d\tau_n \tag{2.2}$$

and other homogeneous functionals of degree less than n whose kernels are derived in a systematic manner from $h_n(\tau_1,\ldots,\tau_n)$, such that for a zero-mean white Gaussian input probe, $x(t)$, G_n is orthogonal to all G-functionals of degree less than n. This can be seen in the first four G-functionals:

$$\begin{aligned}
G_0[h_0,x(t)] &= h_0 \ , \\
G_1[h_1,x(t)] &= \int_{-\infty}^{\infty} h_1(\tau)x(t-\tau)d\tau , \\
G_2[h_2,x(t)] &= \int_{-\infty}^{\infty}\int_{-\infty}^{\infty} h_2(\tau_1,\tau_2)x(t-\tau_1)x(t-\tau_2)d\tau_1 d\tau_2 - K\int_{-\infty}^{\infty} h_2(\tau_1,\tau_1)d\tau_1 , \\
G_3[h_3,x(t)] &= \int_{-\infty}^{\infty}\int_{-\infty}^{\infty}\int_{-\infty}^{\infty} h_3(\tau_1,\tau_2,\tau_3)x(t-\tau_1)x(t-\tau_2)x(t-\tau_3)d\tau_1 d\tau_2 d\tau_3 \\
&\quad -3K\int_{-\infty}^{\infty}\int_{-\infty}^{\infty} h_3(\tau_1,\tau_2,\tau_2)x(t-\tau_1)d\tau_1 d\tau_2 ,
\end{aligned} \tag{2.3}$$

where the power density spectrum of the input probe, $x(t)$, is $\Phi_{xx}(f)=K$.

In this formulation, the Wiener kernels, $\{h_n\}$, completely characterize a time-invariant nonlinear system if its memory asymptotically approaches zero for the infinite past. Due to the orthogonality property of the G-functionals, the Wiener series may be truncated after n G-functionals, giving the best nth order polynomial nonlinear approximation to the system output in the sense of least integral square error. Higher order functionals are independent and can be added later without affecting the estimate of G-functionals already obtained. So the problem of system identification becomes the problem of determining the Wiener kernels.

Wiener accomplished this by expanding the kernels in terms of a set of orthogonal functionals; he used the Laguerre functions in particular. Thus, the identification process is further reduced to determining the coefficients of this expansion. Since the Laguerre functions can be represented by a series of phase-shift electrical networks, the coefficients can be determined by a system of physical measurements. This method is suitable for analog measurements, but it does not readily lend itself to digital computations. Practical considerations require the kernels to be expanded in terms of a finite series, which will introduce truncation errors. Although these errors are minimum integral square errors associated with the expansion on a finite orthogonal set, they are still prohibitive in most practical applications of the Wiener theory.

Lee and Schetzen (1965), however, introduced a method of determining the Wiener kernels which employs a cross-correlation algorithm. It avoids the expansion of the kernels which is essential in Wiener's method, and the kernels can be calculated point by point for simple digital implementation. The method uses a set of functionals that are formed by passing a zero-mean white Gaussian process, x(t), through a system of parallel delay circuits and multiplying their outputs. This yields

$$\begin{aligned} y_n(t) &= x(t-\tau_1)\ldots x(t-\tau_n) \qquad (2.4) \\ &= \int_{-\infty}^{\infty}\cdots\int_{-\infty}^{\infty}\delta(\sigma_1-\tau_1)\ldots\delta(\sigma_n-\tau_n)x(t-\sigma_1)\ldots x(t-\sigma_n)d\sigma_1\ldots d\sigma_n \;. \end{aligned}$$

The integral is a homogeneous functional of nth degree; therefore, the product of $y_n(t)$ and the response of an unknown system to the same x(t) can be averaged to determine the nth-order Wiener kernel, h_n.

Consider an unknown time-invariant nonlinear system, S, with a zero-mean white Gaussian input probe, $x(t)$, and output, $y(t)$. The zeroth-order Wiener kernel, h_0, is simply the time average of the output, $\overline{y(t)}$. The first-order Wiener kernel is measured by applying $x(t)$ to the unknown system which yields $y(t)$ and a delay circuit to form $y_1(t)$. Multiplying $y(t)$ and $y_1(t)$ and averaging the product gives

$$\overline{y(t)y_1(t)} = \overline{\{\sum_{n=0}^{\infty} G_n[h_n,x(t)]\}x(t-\tau)} \ .$$

Since $y_1(t)$ results from a functional of the first degree, the G-functionals, for $n>1$, are orthogonal to $x(t-\tau)$. So we have

$$\overline{y(t)y_1(t)} = \overline{\{\sum_{n=0}^{1} G_n[h_n,x(t)]\}x(t-\tau)} \ .$$

For $n=0$ we have

$$\overline{G_0[h_0,x(t)]x(t-\tau)} = h_0\overline{x(t-\tau)} = 0 \ ,$$

since $x(t)$ is zero-mean. Hence

$$\begin{aligned}
\overline{y(t)y_1(t)} &= \overline{[\int_{-\infty}^{\infty} h_1(\sigma)x(t-\sigma)d\sigma]x(t-\tau)} \\
&= \int_{-\infty}^{\infty} h_1(\sigma)\overline{x(t-\sigma)x(t-\tau_1)}d\sigma \\
&= \int_{-\infty}^{\infty} h_1(\sigma)K\delta(\tau-\sigma)d\sigma \\
&= Kh_1(\tau) \ .
\end{aligned}$$

Therefore, we obtain

$$h_1(\tau) = \frac{1}{K}\overline{y(t)x(t-\tau)} \ . \qquad (2.5)$$

The first-order Wiener kernel, then, is the cross-correlation of the output and input divided by the power level of the input of the unknown system when probed with a zero-mean white Gaussian process.

The second-order Wiener kernel is measured in the same manner:

$$\overline{y(t)y_2(t)} = \overline{\{\sum_{n=0}^{\infty} G_n[h_n,x(t)]\}\, x(t-\tau_1)x(t-\tau_2)} \;,$$

but $y_2(t)$ results from a second degree functional, so

$$\overline{y(t)y_2(t)} = \overline{\{\sum_{n=0}^{2} G_n[h_n,x(t)]\}\, x(t-\tau_1)x(t-\tau_2)} \;.$$

For n=0 we have

$$\overline{G_o[h_o,x(t)]x(t-\tau_1)x(t-\tau_2)} = h_o\overline{x(t-\tau_1)x(t-\tau_2)} = h_oK\delta(\tau_1-\tau_2) \;,$$

and for n=1

$$\begin{aligned}\overline{G_1[h_1,x(t)]x(t-\tau_1)x(t-\tau_2)} &= \overline{[\int_{-\infty}^{\infty} h_1(\sigma)x(t-\sigma)d\sigma]x(t-\tau_1)x(t-\tau_2)} \\ &= \int_{-\infty}^{\infty} h_1(\sigma)\overline{x(t-\sigma)x(t-\tau_1)x(t-\tau_2)}d\sigma \\ &= 0 \;,\end{aligned}$$

since the average of the product of an odd number of zero-mean Gaussian variables is zero. Finally, for n=2

$$\begin{aligned}\overline{G_2[h_2,x(t)]x(t-\tau_1)x(t-\tau_2)} = \Big[&\overline{\int_{-\infty}^{\infty}\int_{-\infty}^{\infty} h_2(\sigma_1,\sigma_2)x(t-\sigma_1)x(t-\sigma_2)d\sigma_1 d\sigma_2} \\ &\overline{-K\int_{-\infty}^{\infty} h_2(\sigma_2,\sigma_2)d\sigma_2\Big]x(t-\tau_1)x(t-\tau_2)}\end{aligned}$$

$$= \int_{-\infty}^{\infty}\int_{-\infty}^{\infty} h_2(\sigma_1,\sigma_2)\overline{x(t-\sigma_1)x(t-\sigma_2)x(t-\tau_1)x(t-\tau_2)}d\sigma_1 d\sigma_2$$

$$-K^2\delta(\tau_1-\tau_2)\int_{-\infty}^{\infty} h_2(\sigma_2,\sigma_2)d\sigma_2$$

$$= K^2[\delta(\tau_1-\tau_2)\int_{-\infty}^{\infty} h_2(\sigma_1,\sigma_1)d\sigma_1 + h_2(\tau_1,\tau_2)$$

$$+ h_2(\tau_2,\tau_1) - \delta(\tau_1-\tau_2)\int_{-\infty}^{\infty} h_2(\sigma_2,\sigma_2)d\sigma_2]$$

$$= 2K^2 h_2(\tau_1,\tau_2) .$$

Therefore

$$\overline{y(t)y_2(t)} = \overline{y(t)x(t-\tau_1)x(t-\tau_2)} = 2K^2 h_2(\tau_1,\tau_2) + h_0 K\delta(\tau_1-\tau_2) ,$$

or

$$h_2(\tau_1,\tau_2) = \frac{1}{2K^2}\overline{y(t)x(t-\tau_1)x(t-\tau_2)} , \text{ for } \tau_1 \neq \tau_2 . \qquad (2.6)$$

The general result for measuring the Wiener kernels is

$$h_n(\tau_1,\ldots,\tau_n) = \frac{1}{n!K^n}\overline{y(t)y_n(t)} = \frac{1}{n!K^n}\overline{y(t)x(t-\tau_1)\ldots x(t-\tau_n)} , \quad (2.7)$$

except when two or more τ's are equal. This final restriction is not severe because we can come arbitrarily close to these points in practical applications. Lee and Schetzen (1965), however, present a method which will remove the restriction with a small amount of difficulty. Take for example eqn. (2.6) where the restriction first appears. The restriction occurs because the second term is assumed to be zero which is not necessarily true when $\tau_1 = \tau_2$. This term results from the G_0 portion of $y(t)$. Since G_0 has already been determined when h_2 is calculated it can be subtracted from $y(t)$ to eliminate the second term. The result is

$$h_2(\tau_1,\tau_2) = \frac{1}{2K^2}\overline{[y(t)-h_o]x(t-\tau_1)x(t-\tau_2)}\ , \tag{2.8}$$

which is valid for all τ_1 and τ_2. In general we have

$$h_n(\tau_1,\ldots,\tau_n) = \frac{1}{n!K^n}\overline{\{y(t)-\sum_{m=0}^{n-1} G_m[h_m,x(t)]\}\ y_n(t)}\ . \tag{2.9}$$

In either case the multidimensional cross-correlations required to determine the kernels are straight forward and simple to program. The Lee and Schetzen algorithm is used to determine the Wiener kernels in this research.

CHAPTER III

ERRORS DUE TO FINITE POWER WHITE NOISE APPROXIMATIONS

The Wiener theory requires that the system to be identified be probed with a zero-mean Gaussian white noise process. Since white noise has infinite power it is impossible to construct such a probe in a physical application of the theory. In practice a white noise process is approximated with a finite power signal that is nearly white over the bandwidth of the system to be identified. However, this approximation leads to errors in the calculated kernels. For digital implementations a piecewise constant independent increment white noise approximation is typically employed. This approximation in particular introduces errors into the calculated Wiener kernels that are dependent upon the bandwidth of the approximation, and for certain types of nonlinearities such as thresholds, the errors also exhibit a dependence upon the power of the white noise approximation. For simple nonlinearities these errors can be described parametrically and by doing so some insight can be gained into how they arise and the effects they have upon the calculated kernels.

The White Noise Approximation

A comprehension of the independent increment white noise process and its implications is essential to understanding these errors. The approximation is rarely discussed; therefore, the following description is presented before continuing. Samples of the process are constructed by randomly choosing values from a zero-mean Gaussian distribution with

variance σ^2, and then holding the process constant equal to this value over an increment in time of length T. Additional points are chosen independently from the Gaussian distributed set. Thus a series of incremental steps with width T and independent zero-mean Gaussianly distributed amplitudes, a_i, is formed:

$$x(t) = \lim_{N\to\infty} \sum_{n=-N}^{N} a_n[u_1(t-nT)-u_1(t-nT-T)], \tag{3.1}$$

where $u_1(t)$ is a generalized step function.

The starting times of the increments in the approximation are not critical in this application as long as their length is always T. Assuming the starting times in different sample functions of the approximation are uniformly distributed over time, the white noise approximation is ergodic. The autocorrelation is

$$R_{xx}(\tau) = \overline{x(t)x(t-\tau)} .$$

Making this calculation gives

$$R_{xx}(\tau) = \overline{\lim_{N\to\infty} \sum_{n=-N}^{N} \sum_{m=-N}^{N} a_n a_m[u_1(t-nT)-u_1(t-nT-T)][u_1(t-mT-\tau)-u_1(t-mT-T-\tau)]}$$

$$= \lim_{N\to\infty} \sum_{n=-N}^{N} \sum_{m=-N}^{N} a_n a_m \overline{[u_1(t-nT)-u_1(t-nT-T)][u_1(t-mT-\tau)-u_1(t-mT-T-\tau)]} .$$

Calculating the area under the product of the step functions and dividing by the total record length (2N+1)T gives

$$R_{xx}(\tau)=\begin{cases}\lim\limits_{N\to\infty}\dfrac{1}{(2N+1)T}\sum\limits_{n=-N}^{N}\sum\limits_{m=-N}^{N}a_na_m[mT+T+\tau-nT], & nT<mT+T+\tau<nT+T\\[2ex] \lim\limits_{N\to\infty}\dfrac{1}{(2N+1)T}\sum\limits_{n=-N}^{N}\sum\limits_{m=-N}^{N}a_na_m[nT+T-(mT+\tau)], & nT<mT+\tau<nT+T\\[2ex] 0,\ \text{elsewhere}\end{cases}$$

$$R_{xx}(\tau)=\begin{cases}\lim\limits_{N\to\infty}\dfrac{1}{(2N+1)T}\sum\limits_{n=-N}^{N}\sum\limits_{m=-N}^{N}a_na_m[T-|mT+\tau-nT|], & |mT+\tau-nT|<T\\[2ex] 0 & , |mT+\tau-nT|\geq T\ .\end{cases}$$

Now let n=i+m, then

$$R_{xx}(\tau)=\begin{cases}\lim\limits_{N\to\infty}\dfrac{1}{(2N+1)T}\sum\limits_{i=N-m}^{N-m}(T-|\tau-iT|)\sum\limits_{m=-N}^{N}a_{i+m}a_m & , |\tau-iT|<T\\[2ex] 0 & , |\tau-iT|\geq T\ .\end{cases}$$

Since a_{i+m} is independent of a_m except when i=0 in which case they are equal,

$\lim\limits_{N\to\infty}\sum\limits_{m=-N}^{N}a_{i+m}a_m = 0$ for $i\neq 0$; therefore we have

$$R_{xx}(\tau)=\begin{cases}\lim\limits_{N\to\infty}\dfrac{1}{(2N+1)T}(T-|\tau|)\sum\limits_{m=-N}^{N}a_m^2, & |\tau|<T\\[2ex] 0 & , |\tau|\geq T\end{cases}$$

$$=\begin{cases}(1-\dfrac{|\tau|}{T})\lim\limits_{N\to\infty}\dfrac{1}{(2N+1)}\sum\limits_{m=-N}^{N}a_m^2 & , |\tau|<T\\[2ex] 0 & , |\tau|\geq T\end{cases}$$

$$R_{xx}(\tau)=\begin{cases}\sigma^2(1-\dfrac{|\tau|}{T}), & |\tau|<T\\[2ex] 0\ , & |\tau|\geq T\ .\end{cases}\qquad(3.2)$$

This is a triangular pulse centered at the origin with amplitude σ^2 and duration 2T. The power spectrum $\Phi(f)$ of the approximation is the Fourier transform of $R_{xx}(\tau)$

$$\Phi(f) = \sigma^2 T \left(\frac{\sin \pi fT}{\pi fT}\right)^2 \tag{3.3}$$

As a check $\Phi(f)$ can be integrated over all frequency. The result is σ^2 which is the expected power of the underlying Gaussian process.

It is not necessary to assume a uniform distribution of the increment starting times to get this result. Assume the starting times are identical for all sample functions of the white noise approximation. In this case the problem is complicated by the fact that the function is no longer ergodic. (It is easily seen that $\langle x(t_1)x(t_2)\rangle$ is not simply a function of t_2-t_1.) To arrive at an expression for the power distribution of the white noise approximation, extended definitions of correlation functions and power spectra which were developed by Lampard (1954) are invoked. Consider the energy spectrum, E(f), of the independent increment white noise approximation up to time t=NT. Now examine the incremental increase in the energy spectrum, $E_T(f)$, that occurs when the process continues to (N+1)T. There is an increase of $a_{N+1}^2 T$, for an average increase of $\sigma^2 T$, in the total process energy every T seconds. The increase is distributed as the energy spectrum of a square pulse with an average amplitude of σ,

$$E_T(f) = \sigma^2 \left(T \frac{\sin \pi fT}{\pi fT}\right)^2 . \tag{3.4}$$

Power can be defined as the time rate of change in energy. By extending this definition to the power and energy spectra and knowing the increase in E(f) is $E_T(f)$ every T seconds, we have

$$\Phi(f) = \frac{E_T(f)}{T} = \sigma^2 T \left(\frac{\sin \pi f T}{\pi f T}\right)^2 .$$

This is the same result as obtained in eqn. (3.3) above. Notice the problem is considered in increments of T, this implies an "incrementally ergodic" function. It is not necessary, however, to use a starting time of NT in determining $E_T(f)$; it is simply convenient to do so.

The half-power points for $\Phi(f)$ are approximately $\pm \frac{1}{2T}$. Choosing T small enough will extend the bandwidth of the approximation to cover the bandwidth of the system under investigation. If this is done, the independent increment process described approximates relative to the unknown system, a zero-mean Gaussian white noise with a power level of $\Phi(0)=\sigma^2 T$. The calculated kernels, therefore, should be normalized with $K=\sigma^2 T$. This expression reveals some of the effects which the white noise approximation has upon the calculated kernels. If σ^2 is taken to infinity and T is taken to zero such that $K=\sigma^2 T$ remains constant, it can be seen from eqn. (3.3) that ideal white noise will be achieved. The expression above can be rearranged to $T=\frac{K}{\sigma^2}$. In this form it can clearly be seen (see Fig. I , T vs. σ^2) that the value of K is arbitrary in determining the Wiener kernels. Taking the limit as σ^2 goes to infinity, or as T goes to zero, they imply the same thing, the lines for various values of K converge on each other. This is reassuring since the development of the Wiener theory does not suggest a dependence of the kernels upon K.

Problems sometimes arise in choosing a value of K, however, in physical applications of the theory. The calculated kernels are actually statistical estimates of the true kernels and they have some variance associated with them. This fact imposes certain restrictions on T which are discussed by Marmarelis (1972). T must be chosen small enough such that the bandwidth of the white noise approximation is greater than the bandwidth of the

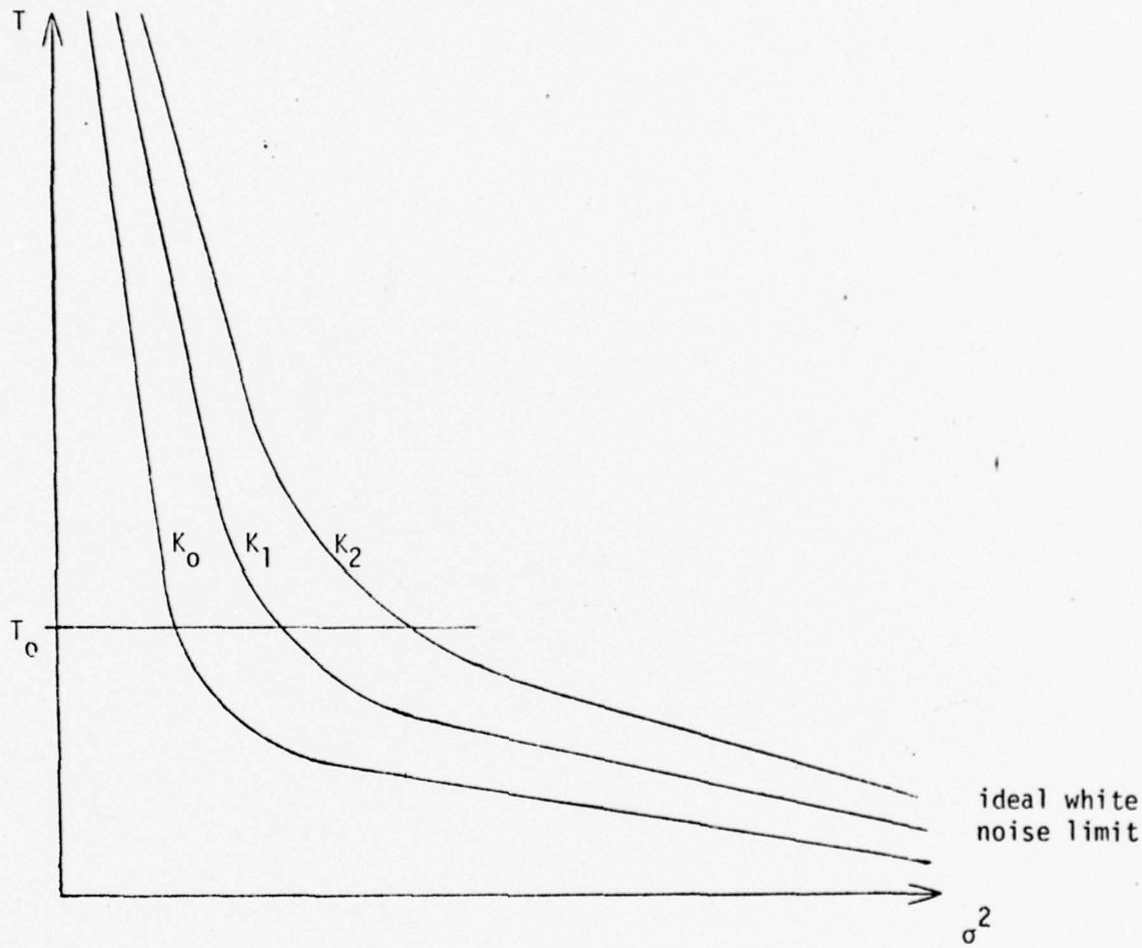

Figure I. Loci of Constant Power White Noise Approximations

unknown system, but if it is chosen too small Marmarelis' work indicates that the variance of the estimated kernels becomes excessive. Therefore, a value for T is usually set early in the identification process. With this constraint on T there is no guarantee that the calculated kernels are independent of the choice of K (see the $T=T_0$ line in Fig. 1). For some nonlinearities such as the simple limiter it can be shown that the calculated kernels are dependent upon K when T is constrained. This in effect means that the calculated kernels are dependent upon the power, σ^2, of the approximate white noise input probe and therefore errors in the calculated kernels are also dependent upon the power of the input probe. Since the instantaneous power of a signal is related to the amplitude of the signal and the errors in the kernels usually become evident as the amplitude of the input to the modeled system is varied, the term amplitude dependent error is used to denote the dependence of the errors upon σ^2.

Amplitude Dependent Error Analysis

The limiter is a graphic example of the dependence of the calculated kernels upon the power of the input probe. Since all physical systems contain a limiter of sorts, it is also a very practical example. Consider the simple ideal limiter:

$$y(t) = \begin{cases} -1 & , x(t) \leq -1 \\ x(t) & , |x(t)| < 1 \\ 1 & , x(t) \geq 1 \end{cases} \quad . \tag{3.5}$$

Let us probe the system with an independent increment white noise approximation, x(t). The zeroth-order Wiener kernels is

$$h_0 = \overline{y(t)} = 0 \; . \tag{3.6}$$

The amplitudes of the different increments of a sample function of $x(t)$ may be viewed as an ensemble of points from the Gaussian distribution. The first-order Wiener kernel is

$$h_1(1) = \frac{1}{K}\,\overline{y(t)x(t-\tau)}$$

$$= \begin{cases} \dfrac{1}{\sigma^2 T}\dfrac{1}{\sqrt{2\pi\sigma^2}}\left[-\displaystyle\int_{-\infty}^{-1} xe^{-x^2/2\sigma^2}dx+\int_{-1}^{1} x^2e^{-x^2/2\sigma^2}dx+\int_{1}^{\infty} xe^{-x^2/2\sigma^2}dx\right]\left[1-\dfrac{|\tau|}{T}\right], & |\tau|<T \\ 0 \quad\cdot & |\tau|\geq T \end{cases}$$

For notational convenience the following triangular pulse is defined:

$$D(\tau) = \begin{cases} \frac{1}{T}[|1-\frac{|\tau|}{T}] \ , & |\tau|<T \\ 0 \ , & |\tau|\geq T \ . \end{cases} \qquad (3.7)$$

Notice that $D(\tau)$ approaches the Dirac delta function as T approaches zero. Combining the integrals gives

$$h_1(\tau) = \frac{2}{\sigma^3\sqrt{2\pi}}\left[\int_0^1 x^2e^{-x^2/2\sigma^2}dx+\int_1^{\infty} xe^{-x^2/2\sigma^2}dx\right] D(\tau) \ .$$

Making a change of variable, $x \rightarrow \frac{x}{\sigma}$, we have

$$h_1(\tau) = \left[\frac{2}{\sqrt{2\pi}}\int_0^{1/\sigma} x^2e^{-x^2/2}\,dx + \frac{2}{\sigma\sqrt{2\pi}}\int_{1/\sigma}^{\infty} xe^{-x^2/2}dx\right] D(\tau) \ .$$

Finally, separating the integral into a form that is commonly tabulated yields

$$h_1(\tau) = \frac{2}{\sqrt{2\pi}}\left[\int_0^{1/\sigma}(x^2-1)e^{-x^2/2}dx+\int_0^{1/\sigma} e^{-x^2/2}dx+\frac{1}{\sigma}\int_{1/\sigma}^{\infty} xe^{-x^2/2}dx\right]D(\tau) \ .$$

The integrand of the first integral is a perfect differential, $d(-xe^{-x^2/2})=(x^2-1)e^{-x^2/2}dx$. The second integral, is the cumulative distribution

function of a standardized Gaussian process, $F(x)$. The integrand of the third integral is also a perfect differential, $d(-e^{-x^2/2})=xe^{-x^2/2}dx$. Therefore, the final result is

$$h_1(\tau) = [2F(\tfrac{1}{\sigma})-1]D(\tau) \quad . \tag{3.8}$$

Since $h_0=0$, from eqn. (2.8) the second-order Wiener kernel is

$$h_2(\tau_1,\tau_2) = \frac{1}{2K^2}\overline{y(t)x(t-\tau_1)x(t-\tau_2)}$$

$$= \begin{cases} \dfrac{1}{2(\sigma^2T)^2}\dfrac{1}{\sqrt{2\pi\sigma^2}}\left[-\int_{-\infty}^{-1}x^2e^{-x^2/2\sigma^2}dx+\int_{-1}^{1}x^3e^{-x^2/2\sigma^2}dx+\int_{1}^{\infty}x^2e^{-x^2/2\sigma^2}dx\right]\left[1-\dfrac{|\tau_1-\tau_2|}{T}\right], \\ |\tau_1-\tau_2|<T \\ 0 \qquad , \quad |\tau_1-\tau_2|\geq T \quad . \end{cases}$$

Combining the integrals yields

$$h_2(\tau_1,\tau_2) = 0 \quad . \tag{3.9}$$

The calculated first-order kernel is obviously dependent upon the choice of σ^2 and T. In general it is difficult to accurately describe these dependencies from experimental data. They are usually complicated and they can change significantly with slight changes in the system configuration. Consider

$$y(t) = \begin{cases} 1-e^{-2x^2(t)} \quad , \quad x(t)>0 \\ -1+e^{-2x^2(t)} \quad , \quad x(t)<0 \quad . \end{cases} \tag{3.10}$$

This is a smooth limiter which approximates the ideal limiter. The kernels are

$$h_o = 0 \tag{3.11}$$

$$h_1(\tau) = \frac{1}{\sigma^2}\frac{1}{\sqrt{2\pi\sigma^2}}\left[\int_{-\infty}^{0}(-1+e^{-2x^2})xe^{-x^2/2\sigma^2}dx+\int_0^{\infty}(1-e^{-2x^2})xe^{-x^2/2\sigma^2}dx\right]D(\tau)$$

$$= \frac{2}{\sigma^3\sqrt{2\pi}}\left[\int_{-\infty}^{0}xe^{-(4\sigma^2+1)x^2/2\sigma^2}dx-\int_{-\infty}^{0}xe^{-x^2/2\sigma^2}dx\right]D(\tau) .$$

Making a change of variable on the first integral of $x \to \sqrt{\frac{4\sigma^2+1}{2\sigma^2}}\,x$ and on the second integral of $x \to \frac{x}{\sigma\sqrt{2}}$ gives

$$h_1(\tau) = \frac{2}{\sigma^3\sqrt{2\pi}}\left[\frac{2\sigma^2}{4\sigma^2+1}\int_{-\infty}^{0}xe^{-x^2}dx-2\sigma^2\int_{-\infty}^{0}xe^{-x^2}dx\right]D(\tau)$$

$$= \frac{4}{\sigma\sqrt{2\pi}}\left(\frac{-4\sigma^2}{4\sigma^2+1}\right)\int_{-\infty}^{0}xe^{-x^2}dx\ D(\tau)$$

$$h_1(\tau) = \frac{8\sigma}{(4\sigma^2+1)\sqrt{2\pi}}D(\tau) \tag{3.12}$$

$$h_2(\tau_1,\tau_2) = \frac{1}{2(\sigma^2T)^2}\frac{1}{\sqrt{2\pi\sigma^2}}\left[\int_{-\infty}^{0}(-1+e^{-2x^2})x^2e^{-x^2/2\sigma^2}dx+\int_0^{\infty}(1-e^{-2x^2})x^2e^{-x^2/2\sigma^2}dx\right]$$
$$D(\tau_1-\tau_2)$$

$$h_2(\tau_1,\tau_2) = 0 . \tag{3.13}$$

Comparing these results with those of the simple limiter, it can be seen that there are large differences between the dependence of the calculated first-order kernel upon the input probe power. The systems are very similar, however. In the limit, as the input approaches white noise the first-order kernels for each limiter goes to zero as $\frac{1}{\sigma}$.

Another problem with identifying the nature of these dependencies can be seen when the simple limiter is assumed to be a physical unknown system to be identified. The power of the input probe must now be

specified. Assume σ^2=0.01 is used; then, the calculated kernels are to four places

$$h_0 = 0$$

$$h_1(\tau) = 1.0000D(\tau)$$

$$h_2(\tau_1,\tau_2) = 0 .$$

Obviously, the kernels would have to be calculated many times, with each calculation providing one point, in determining the kernels dependence upon σ^2 .

The question now arises as to what value of σ^2 should be chosen. The kernels calculated above with σ^2=0.01 predict that the system output is approximately equal to its input (see eqns. (2.1) and (2.3)). This is a valid prediction for inputs which are as small as the input probe. However, for inputs with amplitudes much greater than one, say 10, the prediction, and therefore the calculated kernels, is grossly inaccurate since the output can never exceed one. The amplitude dependent errors, then, are a result of not only the dependence of the calculated kernels upon the input power probe but also of the instantaneous power of system inputs relative to the power of the input probe used to calculate the kernels. The closer they are to each other the better the prediction will be.

The solution to this problem is to use an input probe with a power that is roughly equivalent to the instantaneous power of typical or interesting inputs to the system, but this is not always possible if these values vary significantly. Sometimes wide variations can be tolerated; for example, the kernels of the simple limiter calculated with σ^2=0.01 yield valid predictions of the outputs for any inputs with magnitudes less than 0.1. On the other hand, a very small variation can cause very large errors. Consider the differences in the first-order kernel for the simple

limiter when σ^2 is allowed to vary slightly around one. For $\sigma^2=0.8$, $h_1(\tau)=0.737D(\tau)$, and for $\sigma^2=1.2$, $h_1(\tau)=0.637D(\tau)$. This is a difference of 15.7% for a moderate change in the input probe power. In this case, many sets of kernels would have to be calculated with various values of σ^2 before good accuracy could be achieved in making system output predictions. This approach is the only approach currently available for reducing the significance of these types of amplitude dependent errors in the calculated Wiener kernels.

CHAPTER IV

ERRORS DUE TO FINITE RECORD LENGTHS

The Wiener theory requires that averages implied by the cross-correlations used to calculate the kernels be taken over the interval $(-\infty,\infty)$, but in physical applications these averages can only be taken over a finite interval. This causes errors since the sample means of finite intervals of a random process are not generally equal to the true mean of the process. Unfortunately, this situation is inherent in the kernel calculations. These induced errors are statistical in nature and they can only be estimated. Since Gaussian processes are used to calculate the kernels, the variance of the computed kernels from the true kernels gives a measure of the error.

The manner in which these errors arise can be illustrated with a simple example. Consider a squarer:

$$y(t) = x^2(t) \tag{4.1}$$

This system does not exhibit the amplitude dependent errors discussed in Chapter III. Before calculating the kernels for the squarer the average of an iterated product of a Gaussian random variable is given:

$$\begin{aligned}
\overline{x^n} &= \frac{1}{\sqrt{2\pi\sigma^2}} \int_{-\infty}^{\infty} x^n e^{-x^2/2\sigma^2}\, dx \\
&= \frac{\sigma^n}{\sqrt{2\pi}} \int_{-\infty}^{\infty} x^n e^{-x^2/2}\, dx \\
&= \begin{cases} 0 \quad , \text{ odd } n \\ \sigma^n[1\cdot 3\cdot 5 \ldots (n-1)] \text{ , even } n \text{ .} \end{cases}
\end{aligned} \tag{4.2}$$

For notational convenience the following definition is presented:

$$D(\tau_1,\tau_2) = \begin{cases} \frac{1}{T^2}\left(1-\frac{|\tau_1|}{T}-\frac{|\tau_2|}{T}\right), & -T<\tau_1<0<\tau_2<T \text{ or } -T<\tau_2<0<\tau_1<T \\ \frac{1}{T^2}\left(1-\frac{|\tau_1|}{T}\right), & -T<\tau_1\le\tau_2\le 0 \text{ or } 0\le\tau_2\le\tau_1<T \\ \frac{1}{T^2}\left(1-\frac{|\tau_2|}{T}\right), & -T<\tau_2\le\tau_1\le 0 \text{ or } 0\le\tau_1\le\tau_2<T \\ 0, & \text{elsewhere} \end{cases} \tag{4.3}$$

Notice the similarities to $D(\tau)$ (see eqn. (3.7)); this function is related to two-dimensional cross-correlations of the independent increment white noise approximation, $x(t)$. It is a pyramidal pulse with volume one, and as T approaches zero it approaches a two-dimensional generalization of the Dirac delta function.

The first three Wiener kernels can now be expressed as follows:

$$h_0 = \overline{y(t)} = \overline{x^2(t)} = \overline{x^2} = \sigma^2 \tag{4.4}$$

$$\begin{aligned} h_1(\tau) &= \frac{1}{K}\,\overline{y(t)x(t-\tau)} \\ &= \frac{1}{\sigma^2 T}\,\overline{x^2(t)x(t-\tau)} \\ &= \frac{1}{\sigma^2}\,\overline{x^3}\,D(\tau) \\ &= 0 \end{aligned} \tag{4.5}$$

$$\begin{aligned} h_2(\tau_1,\tau_2) &= \frac{1}{2K}\,\overline{[y(t)-h_0]x(t-\tau_1)x(t-\tau_2)} \\ &= \frac{1}{2(\sigma^2 T)^2}\,\overline{[x^2(t)-\sigma^2]x(t-\tau_1)x(t-\tau_2)} \\ &= \frac{1}{2\sigma^4 T^2}\,[\overline{x^2(t)x(t-\tau_1)x(t-\tau_2)}-\sigma^2\overline{x(t-\tau_1)x(t-\tau_2)}]\ . \end{aligned}$$

Consider the case where $x(t-\tau_1)$ is independent of $x(t-\tau_2)$ but either or both may or may not be independent of $x(t)$. Then we can write the equation as

$$h_2(\tau_1,\tau_2) = \frac{1}{2\sigma^4T^2}\left[\overline{x^2(t)x(t-\tau_1)}\,\overline{x}+\overline{x}\,\overline{x^2(t)x(t-\tau_2)} + \overline{x}^2\,\overline{xx}-\sigma^2\,\overline{xx}\right] = 0 ,$$

since x is a zero-mean process. For the case where $x(t-\tau_1)$ and $x(t-\tau_2)$ are dependent but either or both may be independent of $x(t)$ we have

$$h_2(\tau_1,\tau_2) = \frac{1}{2\sigma^4T^2}\left[\overline{x^2}\;\overline{x(t-\tau_1)x(t-\tau_2)}-\sigma^2\;\overline{x(t-\tau_1)x(t-\tau_2)}\right] = 0 .$$

This leaves the case where $x(t-\tau_1)$, $x(t-\tau_2)$ and $x(t)$ are mutually dependent:

$$\begin{aligned} h_2(\tau_1,\tau_2) &= \frac{1}{2\sigma^4T^2}\left[\overline{x^2(t)x(t-\tau_1)x(t-\tau_2)} - \sigma^2\overline{x(t-\tau_1)x(t-\tau_2)}\right] \\ &= \frac{1}{2\sigma^4}\left[\overline{x^4}-\sigma^2\overline{x^2}\right]D(\tau_1,\tau_2) \\ &= \frac{1}{2\sigma^4}\left[3\sigma^4-\sigma^4\right]D(\tau_1,\tau_2) \\ &= D(\tau_1,\tau_2) \quad . \end{aligned}$$

Summing the contributions of all three cases yields

$$h_2(\tau_1,\tau_2) = D(\tau_1,\tau_2) \quad . \tag{4.6}$$

Remembering that T is assumed to be fixed, the variances of the strengths* of the estimated kernels, denoted by $var[h_i]$, will give a measure of the error in the estimated kernels.

---

*For the continuous time case, the kernels of a simple nonlinear amplifier will consist of impulses; hence the use of the term strength. For our independent increment white noise approximation, the kernel is effectively smeared, and the integral of the smeared kernel equals the strength of the continuous time kernel.

$$\mathrm{var}[h_0] = \frac{1}{M}\,\mathrm{var}[x^2] = \frac{1}{M}\,(\overline{x^4}-\overline{x^2}^2) = \frac{2\sigma^4 T}{L}\,, \tag{4.7}$$

where M is the number of independent samples used to calculate the kernels, which is just L/T where L is the duration of the sample input.

$$\begin{aligned}\mathrm{var}[h_1] &= \frac{1}{M}\,\mathrm{var}[\frac{x^3}{\sigma^2}] \\ &= \frac{1}{M\sigma^4}\,(\overline{x^6} - \overline{x^3}^2) \\ &= \frac{15\sigma^2 T}{L}\quad .\end{aligned} \tag{4.8}$$

$$\begin{aligned}\mathrm{var}[h_2] &= \frac{1}{M}\,\mathrm{var}[\frac{x^4-\sigma^2x^2}{2\sigma^4}] \\ &= \frac{1}{4M\sigma^8}\,(\overline{x^8-2\sigma^2x^6+\sigma^4x^4}-\overline{x^4-\sigma^2x^2}^2) \\ &= \frac{1}{4M\sigma^8}\,(105\sigma^8-30\sigma^8+3\sigma^8-4\sigma^8) \\ &= \frac{37T}{2L}\quad .\end{aligned} \tag{4.9}$$

Viewing eqns. (4.7)-(4.9), some conclusions regarding the accuracy of calculated kernels can be made for simple nonlinear systems such as $y(t)=x^n(t)$ for some integer n. We could continue in a like manner to determine the variance of h_3, h_4, etc. for the case n=2. Doing so shows that $\mathrm{var}[h_m]$ is proportional to $\sigma^{2(2-m)}$. In the general case, $y(t)=x^n(t)$, it is found by a similar analysis that $\mathrm{var}[h_m]$ is proportional to $\sigma^{2(n-m)}$.

We note from eqn. (4.9) that the variance in the estimate of h_2 is independent of σ^2, the power of the input probe, and in general, for $y(t)=x^n(t)$, $\mathrm{var}[h_n]$ will be independent of σ^2. The variances of lower order kernels increase exponentially in σ^2 with a decrease in the order of the kernel, while higher order kernels exhibit a variance that decreases

exponentially in σ^2 with an increase in the order of the kernel.

Thus for a fixed T, the choice of input power σ^2, will greatly effect the accuracy of estimated kernels. It is clear that large σ, $\sigma>1$, will lead to the likelihood of increased error in low order kernels, whereas, small σ, $\sigma<1$, will decrease these errors while increasing the variance of higher order kernels.

The relative exponential increase in σ^2 of the variance of some of the kernels presents a disturbing computational problem. The errors associated with these kernels may be proportionately much larger than that associated with other kernels, as a result of the increased variance. Hence such calculated kernels may seem to contribute significantly more to a modeled system than the true kernels contribute to the underlying true system, leading an experimenter to draw false conclusions about the system under investigation.

This phenomenon may be seen by substituting some numbers into the example of the squarer. Assuming T=1, L=1000 and $\sigma^2=100$ we have $\mathrm{var}[h_0]=20$, $\mathrm{var}[h_1]=1.5$ and $\mathrm{var}[h_2]=\frac{37}{2000}$. Now assuming that there is an error in the calculated kernels of plus one fourth of a standard deviation where $\bar{h}_0=100$ yields

$$h_0 \simeq 101$$

$$h_1(\tau_1) \simeq 0.32\ D(\tau)$$

$$h_2(\tau_1,\tau_2) \simeq 1.032\ D(\tau_1,\tau_2)$$

From eqn. (2.3) these calculated kernels imply an underlying system

$$y(t) = -2.4 + 0.32x(t) + 1.032x^2(t)$$

This system exhibits behavior which is very different from that of the squarer. These values for the kernels would cause approximately a 5% error

in the predicted output from an input with an amplitude equal to 10. This is an instantaneous power of 100 corresponding to the σ^2 used in calculating the kernels. Notice that the error increases as the amplitude of the input decreases from 10. If a third-order kernel had been calculated the error would also increase as the amplitude of the input increases from 10. Therefore, we are still faced, as in Chapter III, with the possibility of having to calculate several sets of kernels using various values of σ^2.

If we were to compute the kernels of the squarer using an independent increment white noise approximation input with $\sigma^2=1$, we find that $var[h_0]=0.002$, $var[h_1]=0.015$, and $var[h_2]=37/2000$. Again assuming an error in each of the kernels of plus one fourth standard deviation, we find

$$h_0 \simeq 1.01$$

$$h_1(\tau) \simeq 0.0032\ D(\tau)$$

$$h_2(\tau_1,\tau_2) \simeq 1.032\ D(\tau_1,\tau_2)$$

Notice that these calculated kernels imply an underlying system

$$y(t) = -0.022 + 0.0032x(t) + 1.032x^2(t)$$

and with these kernels, the error for an input when its amplitude is 1 will be approximately 1.3%. As before, any additional higher order kernels calculated for this system will exhibit errors which increase with increasing amplitude.

From the preceeding material, it is clear that nonlinear systems of the form $y(t)=ax^n(t)$ are most amenable to reduced error calculation of low order kernels if the power of the input probe $x(t)$ is small. While

computationally desirable, this may not always be physically practical. However, higher order calculated kernels will tend to exhibit larger errors as the input probe power is decreased. For systems which are polynomial type

$$y(t) = a_0 + a_1 x(t) + a_2 x^2(t) + \ldots + a_r x^r(t) \ , \qquad (4.10)$$

for some finite integer r, the error analysis becomes vastly more complicated, as errors in the kernels associated with particular iterated products of x(t) may exhibit behavior opposite that of kernels associated with other products of x(t).

Marmarelis (1972) discusses the errors in the calculated kernels associated with finite input record lengths and gives a method for determining the record length L to insure that var[h_i] falls within prescribed bounds. In view of the exponential change in σ^2 of var[h_i], we might also wish to investigate the use of scaling the input probe to achieve more desirable calculated kernels. However, some reflection on this will show that there is no advantage to scaling that is not compensated and cancelled when the calculated kernels resulting from the scaled input probe are themselves rescaled appropriately.

CHAPTER V

PRACTICAL EXAMPLE

Some Wiener kernels were calculated for a seismic energy propagation channel from data which was collected at Eglin Air Force Base, Florida. The experimental arrangement was similar to that of Walker (1976). It consisted of playing low frequency noise at various amplifications through a speaker in order to stimulate the propagation channel. The response of the propagation channel was then detected with a geophone. Several sets of kernels were calculated for input probes at the same amplification as well as at different amplifications.

The noise was produced with a General Radio Company 1381 Random Noise Generator operating in the 2 hertz to 2,000 hertz mode. The noise was then low pass filtered to 200 hertz with a Tektronics FG-502 Function Generator and then amplified with a Sansui 5000A Power Amplifier which had a frequency response from 15 hertz to 20,000 hertz. At this point the signal was recorded on magnetic tape by an Ampex 2200 FM Recorder which had a frequency response of 0 hertz to 40,000 hertz; this record was taken as the input to the system.

In addition to being recorded, the signal was applied to an Altec 416-8A Speaker with a frequency response of 30 hertz to 1600 hertz which was attached to a plywood cabinet. The cabinet had a base of approximately 1½ feet by 3 feet and a height of about 3 feet. The cabinet rested on the ground with the speaker facing a point 20 feet away where a Geospace

Corporation Vertical Axis Geophone (Pat. 3119978) was buried at a depth of 12 inches. The signal produced by the geophone was also recorded on magnetic tape by the Ampex Recorder using a different channel on the same recording head as was used to record the input. This record was taken as the output of the system. When the experiment was completed, the magnetic records were digitized at a rate of 512 samples per second.

Since the geophone does not react when stimulated with a d-c level, the zeroth-order Wiener kernel is known to be zero. The experimenter should always attempt to take advantage of information such as this when making a physical application of the Wiener theory as it will reduce errors in the modeled system. One-half second samples (from $\tau = -\frac{1}{4}$ to $\tau = \frac{1}{4}$) of the first-order Wiener kernel were calculated. To do this a one-half second sample of the output was cross-correlated with a one second sample of the input which began 1/4 second before the output sample began and ended 1/4 second after the output sample ended.

Fig. II shows a first-order kernel calculated for an input noise probe with an rms amplitude of 1/2 volt. Notice the delay caused by the propagation channel. Fig. III is a first-order kernel calculated with different input-output samples with the input probe rms amplitude still equal to 1/2 volt. Fig. IV and Fig. V are first-order kernels calculated for input rms amplitudes of 1 volt and 2 volts respectively. Fig. VI and Fig. VII are different samples of the first-order kernels calculated for an input rms amplitude of 4 volts. All of these figures are scaled the same and are typical of the results obtained in making the kernel calculations.

There was generally more difference between first-order kernels calculated for different input powers than between different samples of first-order kernels calculated for the same input power. This indicates

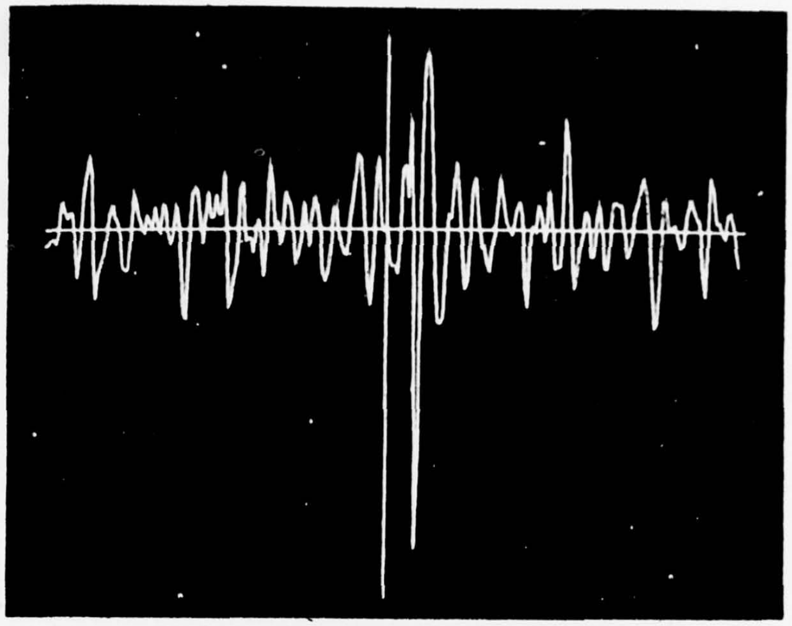

time: $\frac{1}{2}$ second interval $\tau \in [-1/4;1/4]$

input rms amplitude: $\frac{1}{2}$ volt

scale maximum: 5.E-4

scale minimum: -1.E-4

kernel maximum: 4.7501 E-4

kernel minimum: -8.5431 E-4

257 points plotted

Figure II. Calculated first order kernel.

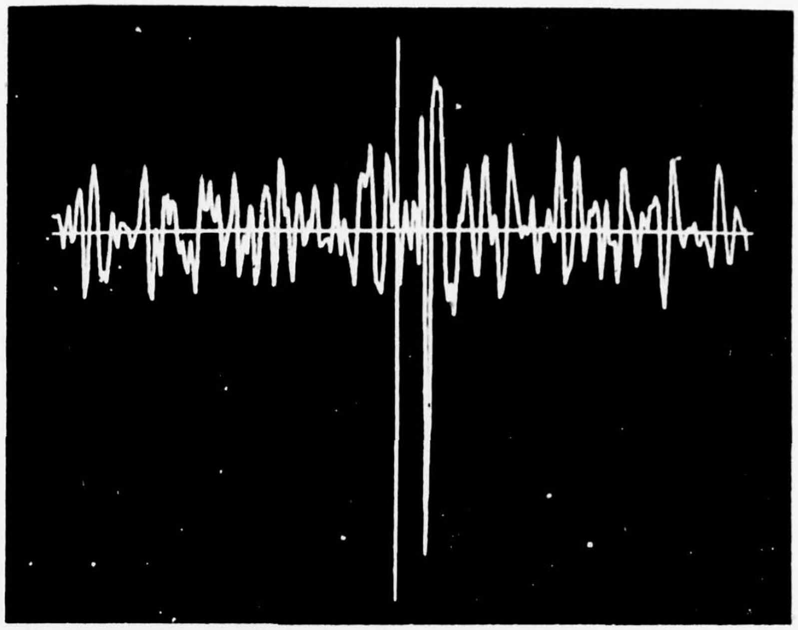

time: $\frac{1}{2}$ second, interval $\tau \epsilon [-1/4, 1/4]$

input rms amplitude: $\frac{1}{2}$ volt

scale maximum: 5.E-4

scale minimum: -1.E-4

kernel maximum: 3.926 E-4

kernel minimum: -8.8127 E-4

257 points plotted

Figure III. Calculated first order kernel.

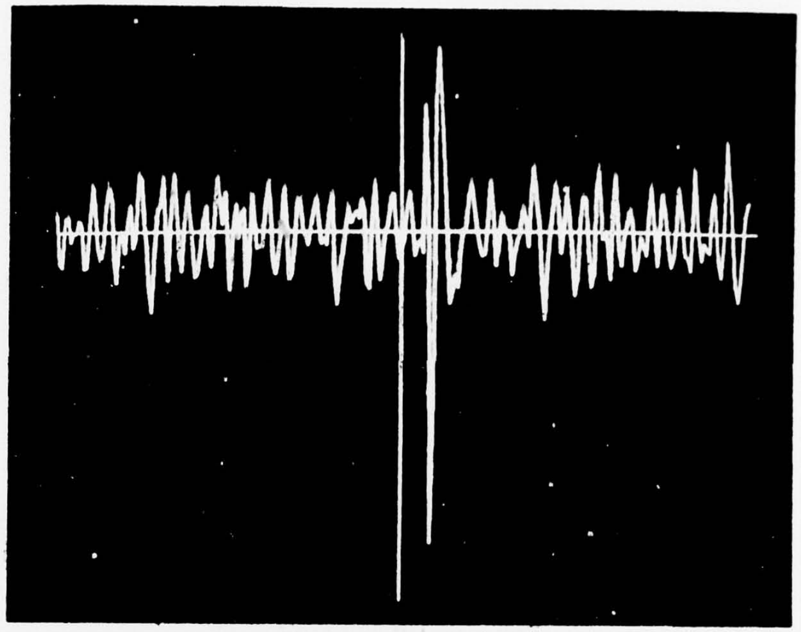

time: $\frac{1}{2}$ secind interval $\tau\epsilon[-1/4,1/4]$

input rms amplitude: 1 volt

scale maximum: 5.E-4

scale minimum: -1.E-4

kernel maximum: 4.9486E-4

kernel minimum: -8.3035E-4

257 points plotted

Figure IV. Calculated first order kernel.

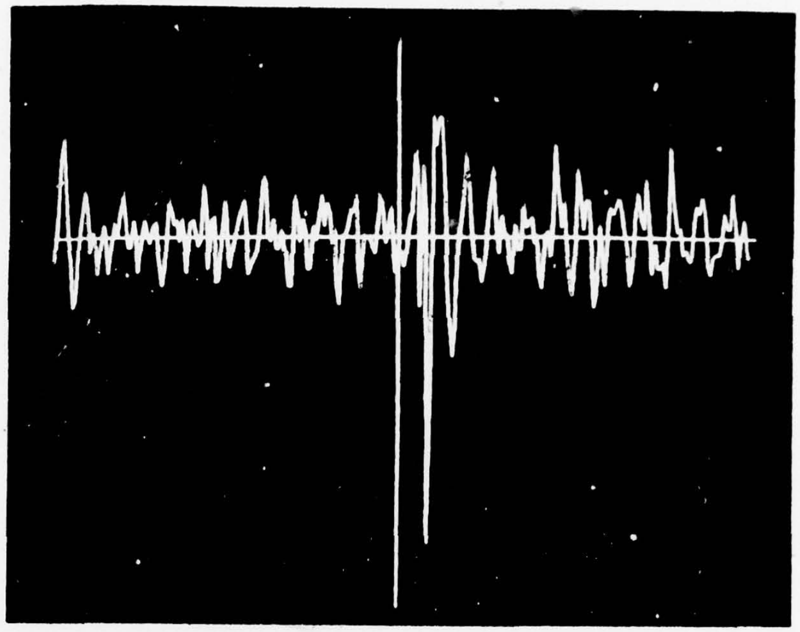

time: $\frac{1}{2}$ second interval $\tau \in [-1/4, 1/4]$

input rms amplitude: 2 volts

scale maximum: 5.E-4

scale minimum: -1.E-4

kernel maximum: 3.1754E-4

kernel minimum: -8.1859E-4

257 points plotted

Figure V. Calculated first order kernel.

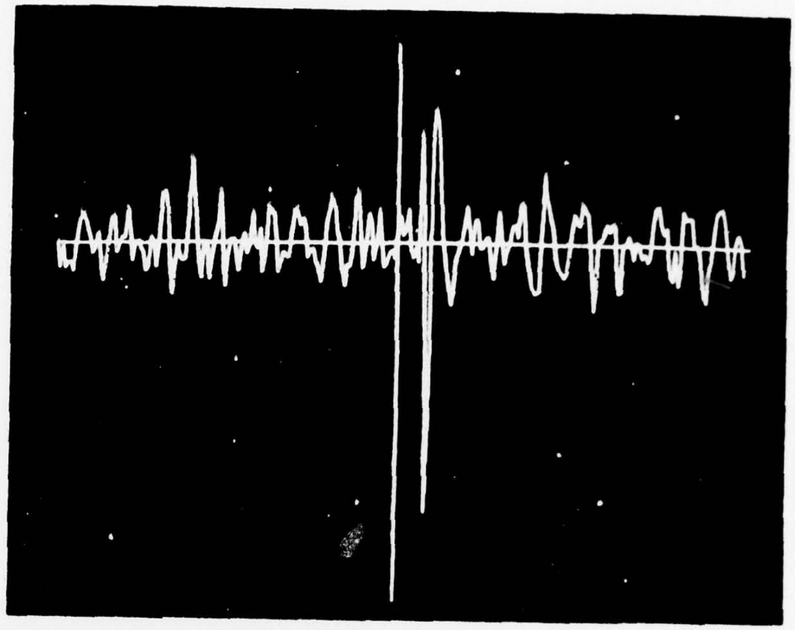

time: $\frac{1}{2}$ second interval $\tau \in [-1/4, 1/4]$

input rms amplitude: 4 volts

scale maximum: 5.E-4

scale minimum: -1.E-4

kernel maximum: 3.6705E-4

kernel minimum: -7.4343E-4

257 points plotted

Figure VI. Calculated first order kernel.

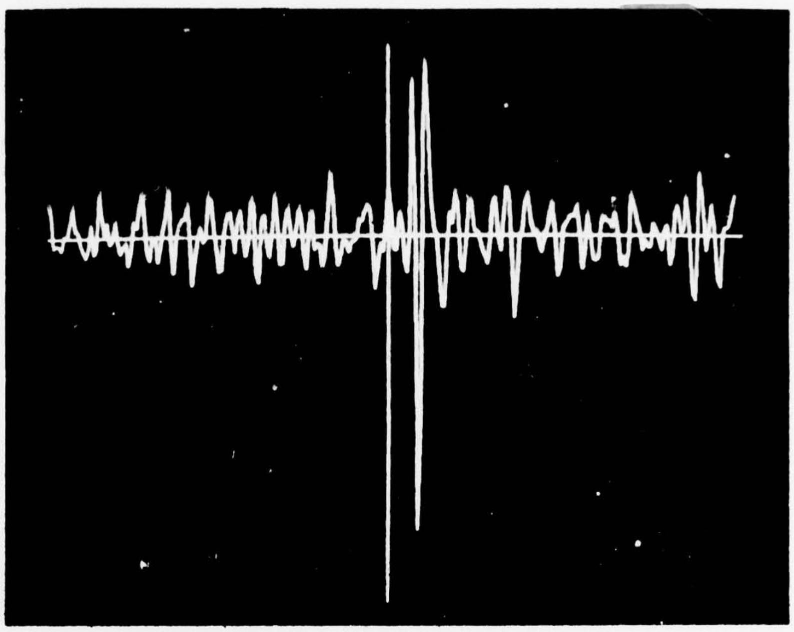

time: $\frac{1}{2}$ second interval $\tau\epsilon[-1/4,1/4]$

input rms amplitude: 4 volts

scale maximum: 5.E-4

scale minimum: -1.E-4

kernel maximum: 4.6190E-4

kernel minimum: -7.9385E-4

257 points plotted

Figure VII. Calculated first order kernel.

the presence of the type of amplitude dependent errors discussed in Chapter III. Furthermore, there was a greater variation in the first-order kernels calculated for larger input power than there was in the first-order kernels calculated with smaller input power. This indicates the presence of the type of amplitude dependent errors discussed in Chapter IV. Neither of these variations are great, however, and it may be possible to ignore them over this range of input amplitudes. This would have to be tested by making output predictions with the various kernels and noting whether or not the variations in the predictions are much larger than the desired accuracy.

Second-order kernels were also calculated. However, due to the long computational time involved in making the calculations and the lack of adequate two-dimensional plotting techniques, an insufficient number of samples of the second-order kernels were obtained to state any conclusive results. The calculated second-order kernels did change with the input probe power, but whether or not the changes were significant or displayed a pattern could not be determined.

CHAPTER VI

SUMMARY

The Wiener theory requires a system which is to be identified to be probed with a zero-mean Gaussian white process. Practical considerations in physical applications of the theory, however, require that approximations of this input probe be made. This leads to errors which sometimes exhibit dependencies upon the power of the approximation.

It was shown in Chapter III that approximating a true white process which has infinite power with a finite power process may result in such amplitude dependent errors in the calculated kernels. It was here that the distinction was made between the power, σ^2, of the physical input probe and the power level, K, of the zero-mean Gaussian white process it is approximating. It was noted that the true kernels are independent of K but the calculated kernels may still depend upon σ^2. The resultant amplitude dependent errors were found to be associated with certain nonlinearities such as thresholds and they can be described for some simple cases. They were shown for the particular case of a limiter.

It was shown in Chapter IV that approximating a true white process which has infinite length with a finite length process may also result in amplitude dependent errors in the calculated kernels. These errors are due to the fact that sample means of a random process over finite intervals are not generally equal to the true mean of the process. Since averages of random processes are inherent in the calculation of the Wiener kernels

the calculated kernels are only statistical estimates of the true kernels. The variance of the estimated kernels gives a measure of their accuracy. The variance can be estimated for simple nonlinearities, and this was done for a squarer. It was seen for the more general system $y(t)=x^n(t)$, that the variances of the kernels is proportional to $\sigma^{2(n-m)}$, where m is the order of the calculated kernel.

If the nonlinearities are only slightly more complicated than those which were discussed, error analysis using the methods employed here would be practically impossible. Therefore, general results can not really be obtained. The experimenter must simply be aware that amplitude dependent errors do occur in the calculated Wiener kernels and attempt to ascertain the extent of their effect on the kernels for each individual system investigated. Currently the only method available for accomplishing this is to calculate several sets of kernels using different values of σ which fall within the amplitude range of relevant inputs to the system and noting any changes which occur between various sets of the calculated kernels.

Note also that none of the simple nonlinearities which were examined had memory and all had infinite bandwidths. To get a better feel for how the amplitude dependent errors affect the calculated kernels of a physical system both of these restrictions should have been avoided. Doing so, however, vastly complicates the problem and simply was not practical in this analysis. There is an obvious need for better means of assessing amplitude dependent errors parametrically with the bandwidth, memory, and dynamic range of the system. Also, extending this analysis into the frequency domain may prove useful in physical applications of the Wiener theory.

REFERENCES

Brownell, W.E., Dept. of Neuroscience and Surgery, University of Florida, personal communications with D.H. Fender, Dept. of Communication Sciences, California Institute of Technology, 1976.

French, A.S. and Butz, E.G., "Measuring the Wiener Kernels of a Nonlinear System Using the Fast Fourier Transform," Int. J. Control, Vol. 17, No. 3, 1973, pp. 529-539.

Krausz, H.I., "Identification of Nonlinear Systems Using Random Impulse Train Inputs," Bio. Cybernetics, Vol. 19, No. 4, 1975, pp. 217-230.

Lampard, D.G., "Generalization of the Wiener-Khintchine Theorem to Nonstationary Processes," J. Appl. Physics, Vol. 25, No. 6, 1953, pp. 802-803.

Lee, Y.W., "Contributions of Norbert Wiener to Linear Theory and Nonlinear Theory in Engineering," from Selected Papers of Norbert Wiener, S.I.A.M. and M.I.T. Press, Cambridge, 1964, pp. 17-33.

Lee, Y.W., Statistical Theory of Communications, Wiley, New York, 1960.

Lee, Y.W. and Schetzen, M., "Measurement of the Wiener Kernels of a Nonlinear System by Cross-Correlation," Int. J. Control, Vol. 2, 1965, pp. 237-254.

Marmarelis, P.Z., "Nonlinear Identification of Bioneuronal Systems Through White-Noise Stimulation," Proceedings of the Joint Automatic Control Conference, Stanford University, August 1972, pp. 117-126.

Raemer, H.R., Statistical Communication Theory and Applications, Prentice Hall, Englewood Cliffs, New Jersey, 1969.

Schetzen, M., "A Theory of Non-Linear System Identification," Int. J. Control, Vol. 20, No. 4, 1974, pp. 577-592.

Volterra, V., The Theory of Functionals and Integro-Differential Equations, Blackie, London, 1930.

Walker, R.B., "Characterization of the Seismic Medium Using Nonlinear Identification Techniques," Engineer Thesis, Dept. of Electrical Engineering, University of Florida, 1976.

White, J.E., Seismic Waves: Radiation, Transmission, and Attenuation, McGraw-Hill, New York, 1965.

Wiener, N., Nonlinear Problems in Random Theory, M.I.T. Press, Cambridge, 1958.